D. Fritsch, M. Englich & M. Sester, eds, 'IAPRS', Vol. 32/4, ISPRS Commission IV Symposium on GIS - Between Visions and Applications, Stuttgart, Germany.

REVISION OF BUILT-UP AREAS IN A GIS USING SATELLITE IMAGERY AND GIS DATA

Andreas Busch
Federal Agency for Cartography and Geodesy
Richard-Strauss-Allee 11
D 60598 Frankfurt am Main, Germany
e-mail: busch@ifag.de, WWW: http://www.ifag.de

KEY WORDS: GIS Update, Small-Scale, Image Analysis, Texture, Linear Feature, Point Detection

ABSTRACT

In general, built-up areas or populated places are significantly changing within the revision interval of a GIS (Geographic Information System) or map. In this paper we present a method by means of which built-up areas are extracted from panchromatic satellite images of SPOT and IRS-1C and which makes use of the available information about built-up areas in the GIS. The method has been developed for small-scale maps or GIS where built-up areas are represented by their outline stored as a closed polygon. The texture of built-up areas in satellite images is characterized by a high spatial density of very short linear features. This density is used to classify built-up and non-built-up areas. The decision is made by a threshold estimated from training sites which are derived from the built-up areas stored in the GIS. The suitability of the method is demonstrated using SPOT and IRS-1C data as examples.

1 INTRODUCTION

1.1 Background

Current research efforts towards using digital images to automize the acquisition and revision of GIS data focus on man-made objects, since they are a matter of rapid change. An overview of the activities and the present state of the art is given by Grün et al., 1997. The main work centres on automatic building extraction from aerial images, where the roofs of the houses are clearly visible. There are only few publications dealing with satellite imagery like TM, SPOT, or IRS-1C serving to detect built-up areas. Obviously, it is not possible to detect single houses in these images. But this is not necessary, since the goal is to support the updating of small-scale maps or GIS where only the outline of built-up areas is stored and not single houses. In the images of the satellites mentioned above built-up areas are represented as a typical texture that is strongly granulated. Thus, purely multispectral classification is not suitable for this purpose. It would fail because of the different spectral characteristics of the varying surfaces that are found in settlements. Due to the size of the pixels, which is of the same order as the size of the objects, different surfaces like roofs, vegetation, and roads contribute to a single pixel. This results in a lot of mixed pixels. Nevertheless, multispectral classification can be used as one source of information, if other features are also taken into account and combined in a knowledge-based system (Vögtle and Schilling, 1995, Schilling and Vögtle, 1997).

Texture is the characterizing feature of built-up areas in satellite imagery. Modelling, synthesis, description, and segmentation of texture are fields of intensive research in computer vision. Texture has its own entry in surveys of the literature on image analysis (e.g. Rosenfeld, 1998) . A series of methods for solving tasks like texture description, texture classification, and texture-based segmentation has been developed. Nevertheless, there is as yet no overall solution for any of these topics due to the variety of different types of texture. Simple techniques like statistical approaches which use moments of the grey levels in an image window have the disadvantage that parameters like mean and variance are independent of the order of the pixels considered. So they are successful under certain conditions only. Better results are obtained by grey level co-occurrence matrices (Haralick and Shapiro, 1992, vol.1, p.457, Lohmann, 1994, Rotunno et al., 1996). Another group of methods is characterized by autoregressive models or by Markov Random Fields (Koch and Schmidt, 1994, p.320, Pan, 1994, Andrey and Tarroux, 1996). Among the spectral approaches especially the wavelet transformation has proved to be suitable for texture segmentation (Shao and Förstner, 1994, Xie and Brady, 1996).

The application of texture analysis to satellite images is tackled as a general segmentation problem (e.g. Lohmann, 1991, Mecocci et al., 1995) or by methods that are designed for special tasks like the extraction of built-up areas (Schilling and Vögtle, 1996, Kunz et al., 1997, Busch, 1997). Because of the timeliness and geometric accuracy of satellite images their use within the revision process of small-scale maps or GIS has advantages as compared to the classical method of updating small scale-maps on the basis of maps of a larger scale (Hanke and Proß, 1994, Konecny, 1996). In addition, automatic cartographic generalization is still unsolved, since solutions are available for special problems only (Burghardt and Meier, 1997).

1.2 Objectives

We want to present a method by means of which built-up areas are extracted from panchromatic satellite images of SPOT and IRS-1C automatically. The approach is based on the results of an earlier paper (Busch, 1997). Now we intend to make use of the information about built-up areas that is already stored in the GIS. Within the scope of small-scale GIS we have do deal with geometric distortions due to generalization and replacement, especially if the GIS data have been derived by digitizing small-scale maps. Automated methods for extracting features from images by means of GIS data have to take into account these geometric distortions. Other systematic effects are caused by the fact that built-up areas will usually grow and that small towns or villages are represented in the GIS by a symbol, e.g. a small circle, that does not cover their whole area. Automation is another important aspect of this paper. Our goal is to avoid control parameters that depend on the image data. Control parameters should be clearly interpretable and have a certain relation to, e.g. map accuracy standards.

2 BASIC IDEAS

2.1 How Do Built-Up Areas Look Like in Satellite Imagery?

Panchromatic satellite images of SPOT and IRS-1C with a ground resolution of 10 and 5.8 meters, respectivly, reproduce built-up areas as a typical texture (Fig. 1). Since the size of most objects in built-up areas like roads, houses, and trees is of the same order as the size of the pixels, it is not possible to identify these objects uniquely and completely. When the extraction of linear features, i.e. lines and edges, is applied to satellite images, the results show

D. Fritsch, M. Englich & M. Sester, eds, 'IAPRS', Vol. 32/4, ISPRS Commission IV Symposium on GIS - Between Visions and Applications, Stuttgart, Germany.

Figure 1: Detail of a SPOT HRV scene.

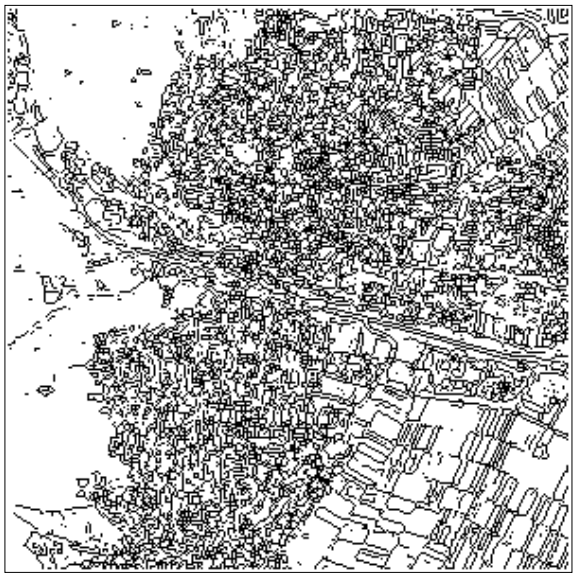

Figure 2: Edges extracted from Fig. 1.

a high spatial density of linear features inside cities. Due to the texture the majority of the extracted lines or edges has a length of a few pixels only. Long structures mostly occur outside of built-up areas, e.g. field boundaries or roads, and they are rare within built-up areas (Fig. 2). Hence, if long linear features are eliminated, the remaining short linear features provide a meaningful criterion for the extraction of built-up areas (Fig. 3).

2.2 Extraction of Lines, Edges, and Points

Since our method for detecting built-up areas in satellite images takes linear features as a starting point, an adequate feature extraction algorithm is required for pre-processing. Any method for edge or line extraction that provides chains of linear feature pixels and stores also their length as an attribute may be used for this purpose. We use an analytic model for extracting lines and edges that is based on the facet model (Haralick, 1984). It has been extended by an approach for noise estimation (Busch, 1996), so that it requires only two simple input parameters, namely the size of an image window and the level of significance for a statistical test. The method allows the extraction of significant points, too. They are interpreted as very short lines, where the directions of maximal and

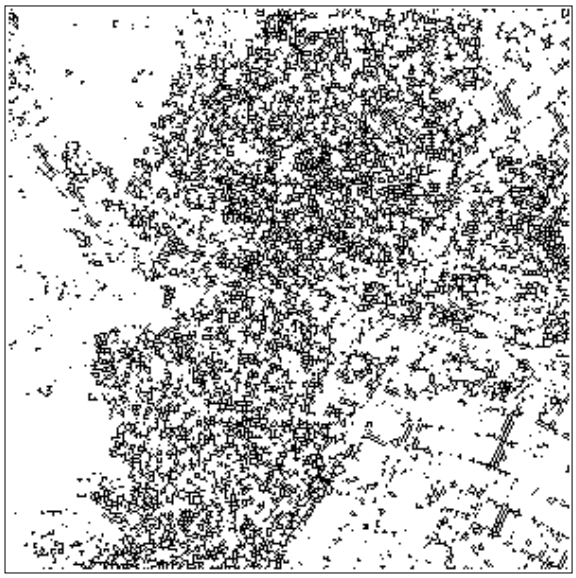

Figure 3: Short edges selected from Fig. 2, length < 3 pixels.

minimal curvature fulfill a certain relation.

For extracing points we make use of the line model

$$g(x,y) = k_0 + k_1 x + k_2 y + k_3 x^2 + k_4 xy + k_5 y^2 \ . \tag{1}$$

It is a polynomial function of the row and column coordinates x and y in an image window of a size of 3×3, 5×5, 7×7, ... pixels. We determine the coefficients $k_0, \ldots, k_5$ from a least squares fit of $g(x,y)$ to the grey values in the image window. The directions of minimal and maximal absolute curvature of the polynomial are obtained from the Hessian $\mathbf{H}$, which is the matrix of second derivatives calculated at the centre of the image window:

$$\mathbf{H} = \left(\begin{array}{cc} \frac{\partial^2 g(x,y)}{\partial x^2} & \frac{\partial^2 g(x,y)}{\partial x \partial y} \\ \frac{\partial^2 g(x,y)}{\partial y \partial x} & \frac{\partial^2 g(x,y)}{\partial y^2} \end{array} \right)_{\substack{x=0 \\ y=0}} = \left(\begin{array}{cc} 2k_3 & k_4 \\ k_4 & 2k_5 \end{array} \right) . \tag{2}$$

The longest eigenvector of $\mathbf{H}$ — with respect to the Euclidian norm — points to the polynomial's direction of maximal absolute curvature. Its direction angle $\alpha \in [0, \pi)$ counting clockwise from the column axis is given by

$$\alpha = \begin{cases} \frac{1}{2} \arctan \frac{k_4}{k_5 - k_3} & \text{if } |k_3| < |k_5| \\ \frac{\pi}{2} + \frac{1}{2} \arctan \frac{k_4}{k_5 - k_3} & \text{if } |k_3| > |k_5| \end{cases} \tag{3}$$

and

$$\alpha = \begin{cases} \pi/4 & \text{if sgn } k_3 = \text{sgn } k_4 \ \wedge \ k_3 = k_5 \\ 3\pi/4 & \text{if sgn } k_3 \neq \text{sgn } k_4 \ \wedge \ k_3 = k_5 \\ \text{undefined} & \text{if } k_4 = 0 \ \wedge \ k_3 = k_5 \\ \text{ambiguous} & \text{if } k_3 = -k_5 \end{cases} . \tag{4}$$

In case of ambiguity both solutions agree with (3). Applying the directional derivative (Haralick, 1984) yields the maximal curvature (Busch, 1994)

$$c_{\max} = k_3 \sin^2 \alpha + k_4 \sin \alpha \cos \alpha + k_5 \cos^2 \alpha \ . \tag{5}$$

D. Fritsch, M. Englich & M. Sester, eds, 'IAPRS', Vol. 32/4, ISPRS Commission IV Symposium on GIS - Between Visions and Applications, Stuttgart, Germany.

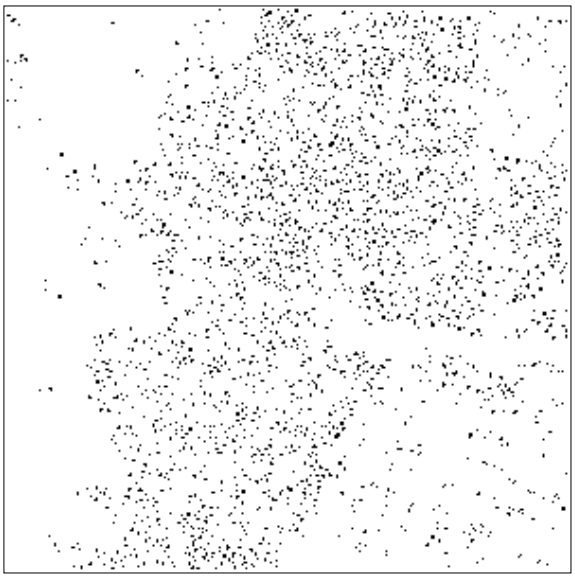

Figure 4: Points extracted from Fig. 1.

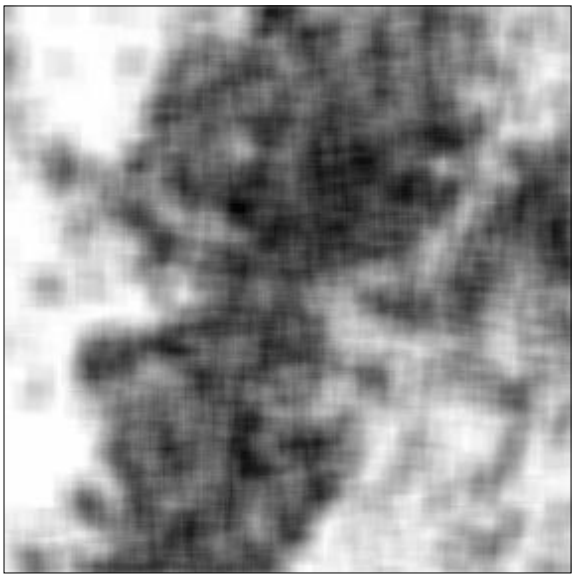

Figure 5: Edge density from Fig. 2 using a 15×15 window.

The orthogonal direction

$$\beta = \alpha + \frac{\pi}{2} \tag{6}$$

furnishes the minimal curvature

$$c_{\text{min}} = k_3 \sin^2 \beta + k_4 \sin \beta \cos \beta + k_5 \cos^2 \beta \ . \tag{7}$$

The fraction

$$f = \frac{|c_{\text{min}}|}{|c_{\text{max}}|} \in [0, 1] \tag{8}$$

measures the compactness of the extracted points. If $f = 1$, the point is perfectly round. Smaller values of f indicate more elongated structures. The signs of c_{min} and c_{max} allow to discriminate peaks, i.e. local maxima, pits, i.e. local minima, and saddle points. Since we are applying the noise estimation mentioned above, only significant points are detected. Thus, the result is not as sensitive to noise as simple techniques for locating local extrema. For our purpose the use of points (Fig. 4) is superior to short linear features, because the length of linear structures is not uniquely defined in dense areas, due to many nodes, links and intersections of the linear features. Other methods for detecting points (Förstner, 1991, p.40) may be suited for our applications, too.

2.3 Densities of Points and Linear Features

Given a binary image indicating that a pixel has a special feature or meets a special condition, we define the feature density as the number of pixels matching this feature that are contained in an image window. For a certain window size we determine the feature density for each pixel in an image. Thus, the result is again an image which we call feature density image (Fig. 5). Within the scope of this paper we use window sizes of 15×15 and 25×25 pixels. Since we calculate the feature density for each pixel, the feature density image has the same resolution as the original one. Hence, we are not losing anything of the original resolution. But their will be effects of smoothing due to the large window size.

The size of the window should be chosen with respect to the following criteria:

- The window size has to be large enough to cover the characteristic structures of the texture.
- The window size has to be large enough to contain a significant number of feature pixels.
- Problems may come up if the number of counted feature pixels is too large to be stored using one byte for each pixel of the feature density image. So one should check for the maximal feature pixel count and either scale it down or use more than one byte per pixel, if necessary.

The application of an appropriate threshold to the feature density image allows to select areas of a high density which correspond to built-up areas.

3 CLASSIFICATION OF BUILT-UP AREAS

The decision whether a pixel is classified as belonging to built-up or non-built-up areas is made by a threshold, which is a very simple method. In this section our objective is to determine the threshold automatically using the information about built-up areas that is already stored in the GIS and to rate the quality of the classification process using distributions derived from the GIS and image data.

3.1 Training Areas Derived from a GIS

When using satellite images and small-scale GIS data or maps for the revision of just that very data, the state depicted in the image and the state documented by the data must differ, because otherwise the images would be unsuited for the update of these data. Therefore, automated methods for analysing images by means of GIS data have to be robust with respect to the differences of the GIS data and the content of the image. Reasons for the differences are given in the following list:

- The information in a small-scale GIS is generalized and there may be local geometric distortions, especially if the GIS data have been derived by digitizing or scanning small-scale maps.
- Built-up areas will usually grow within the update interval.
- Small towns or villages are represented in the GIS by a symbol, e.g. a small circle, that does not cover their whole area.
- Large parks, cemeteries, and sports grounds do not have the same appearance as built-up areas in the satellite image, but may appear as built-up areas in the GIS, if they are located inside a city.

D. Fritsch, M. Englich & M. Sester, eds, 'IAPRS', Vol. 32/4, ISPRS Commission IV Symposium on GIS - Between Visions and Applications, Stuttgart, Germany.

Figure 6: Populated places (black) from a small-scale GIS.

Figure 7: Training sites (black) for built-up areas derived from Fig. 6 by morphological erosion.

From the GIS data (Fig. 6) we generate two sets of training sites, one for the built-up areas and one for the non-built-up areas. The training sites for the built-up areas are produced from the populated places stored in the GIS, but they are reduced in size, i.e. a margin along their outline is deleted (Fig. 7). The width of the margin depends on the size of the geometric distortions of the GIS data. This shrinking operation can be done in an image processing system by using morphological filters, or in a GIS system by a buffer function. To generate the training sites for the non-built-up areas the populated places stored in the GIS are expanded to ensure that the enlarged sites cover the area influenced by geometric distortions and by the growth of the built-up areas since the last data revision. This enlargement must be done for populated places that are stored by a symbol only, too (Fig. 8). Again, the tools used are morphological filters or a buffer function. All sites that are not covered by the enlarged populated places taken from the GIS serve as training sites for the non-built-up areas (Fig. 9).

The size of the enlargement or shrinking depends on several parameters, e.g. the geometric accuracy of the GIS or map, the expected rate of change since the last revision of the data, and map standards. The objective of the creation of the training sets is to obtain training sets that represent one class only and that are influenced as little as possible by the other class.

3.2 Estimation of the Threshold

The distributions or histograms of the feature densities for both types of training sites are analyzed to select an optimal threshold. Fig. 10 shows examples of such histograms obtained from the

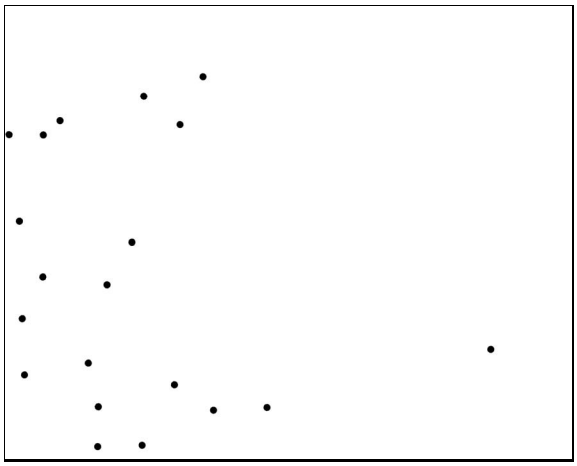

Figure 8: Symbols (black) for small towns and villages from a small-scale GIS.

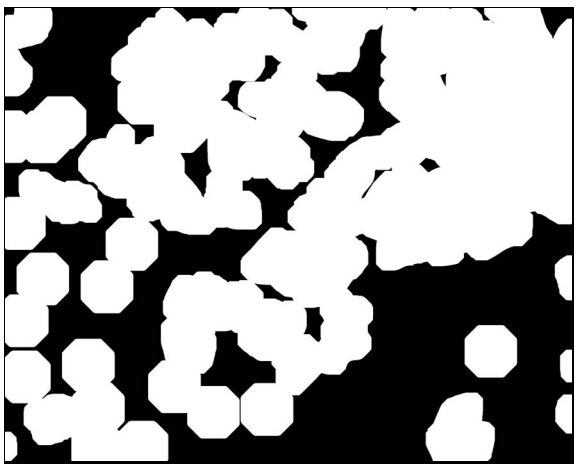

Figure 9: Training sites (black) for non-built-up areas derived from Figs. 6 and 8 by morphological dilation and inversion of the resulting binary image.

D. Fritsch, M. Englich & M. Sester, eds, 'IAPRS', Vol. 32/4, ISPRS Commission IV Symposium on GIS - Between Visions and Applications, Stuttgart, Germany.

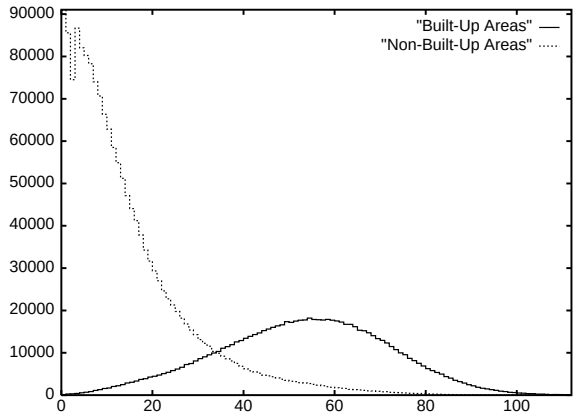

Figure 10: Feature density histograms for built-up and non-built-up areas derived from SPOT data and training sites.

SPOT data of Fig. 11 and the training sites from Figs. 7 and 9. It is possible to use the actual pixel counts without normalizing them, which will provide an optimal threshold for just that set of training sites. Normalization of the histograms supplies distributions which will yield thresholds that are independent of the ratio of the areas covered by both training sites. For estimating the threshold we can use on the one hand the point of intersection of the histograms or distributions, or on the other hand the point where the cumulative histograms or distributions intersect.

3.3 Post-Processing

The results obtained by the method so far can be improved by some steps of post-processing, which are connected to the standards for the production of the particular GIS data or map. So we eliminate blobs of detected built-up areas that are too small to be represented in the GIS or map. Accordingly, small holes within regions of detected built-up areas are filled. The maximal size of the filled or eliminated regions depends on the scale and type of the GIS or map. Another optional step to simplify the results is the approximation of the borders of the extracted regions by straight lines. This may be interpreted as a simple cartographic generalization step.

4 EXAMPLES

4.1 SPOT Data

The data of this example come from a SPOT HRV scene of February 22, 1992, with 10m$\times$10m pixels. Fig. 11 shows the part of the scene that covers our test site. The training sites for built-up and non-built-up areas are depicted in Figs. 7 and 9. From the SPOT data we have extracted edges and then deleted those of a length of more than 3 pixels. We have determined the density of the remaining short edges using a window size of 15$\times$15 pixels. The result of applying 36 as a threshold, which has been obtained from Fig. 10, is documented by Fig. 12. Eliminating small regions and the filling of small holes up to a size of 2000 pixels leads to Fig. 13. In Fig. 14 the result is compared to the GIS data. It demonstrates that all populated places have been detected. There is only one dot from the GIS data at the left margin the corresponding region of which has been eliminated due to its small size which is caused by the fact that it has been truncated by the border of the image. Large regions at the airport in the lower left quadrant of the image have been correctly detected as built-up areas. But they are not stored in the GIS as populated places, which is correct, too. Hence, this discrepancy is a consequence of the different definitions of populated places as stored in the GIS and built-up areas as extracted by our method. A detail of the result is given by Fig. 15. It illustrates the accuracy of the method and its suitability for GIS update.

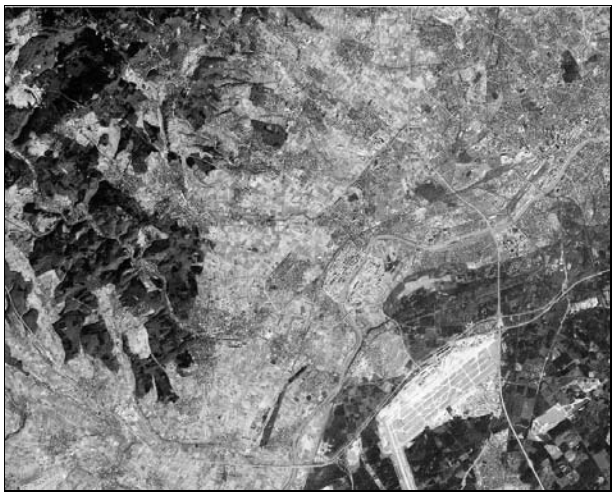

Figure 11: Part of a SPOT scene (2500$\times$2000 pixels) showing a site close to of Frankfurt am Main.

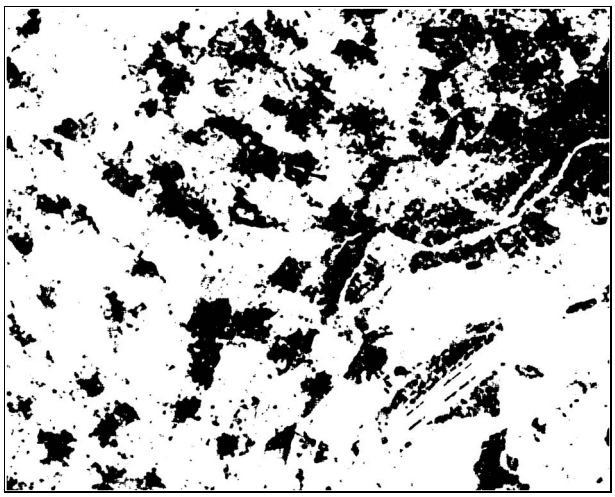

Figure 12: Result of applying a threshold to an edge density image.

The horizontal boundaries of the detected built-up areas appear, because the detail is located at the lower margin of the image.

4.2 IRS-1C Data

For this example we have processed data of the Indian satellite IRS-1C, namely panchromatic data of 5.8m$\times$5.8m ground resolution recorded on April 24, 1997 (Fig. 16). Again, we have used Figs. 6–9 for training and reference. We have extracted points (Fig. 17), where the parameter f from Eq. (8) has been set to 01. A point density image has been derived based on a 25$\times$25 pixel window. The histograms of Fig. 18 visualize the rate of misclassification to be expected, and the selection of the threshold which is 59. Fig. 19 shows the overall results after the filling of small holes and the elimination of small regions. A detail of the results underlaid with the image data is depicted in Fig. 20.

5 CONCLUSIONS AND OUTLOOK

The results of this paper demonstrate that the comparatively simple approach of using feature densities and a threshold for detecting built-up areas works very promisingly. The results are better than the demands on small-scale GIS or maps, so that they are suitable for medium-scale applications, too. The main advantages of our method consist in the estimation of the threshold and the prediction of the quality of the results by means of the histograms for built-up and non-built-up areas.

D. Fritsch, M. Englich & M. Sester, eds, 'IAPRS', Vol. 32/4, ISPRS Commission IV Symposium on GIS - Between Visions and Applications, Stuttgart, Germany.

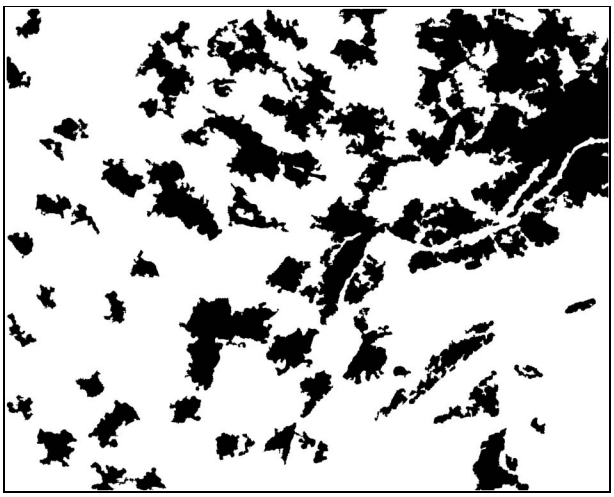

Figure 13: Result after the filling of small holes and the elimination of small regions.

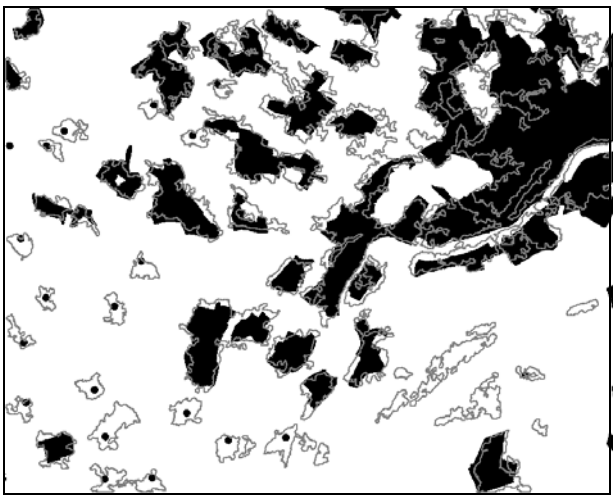

Figure 14: Detected built-up areas (grey) obtained from Fig. 13 and the GIS data (black).

Figure 15: Detail of Fig. 11 with detected built-up areas (white) and GIS data (black).

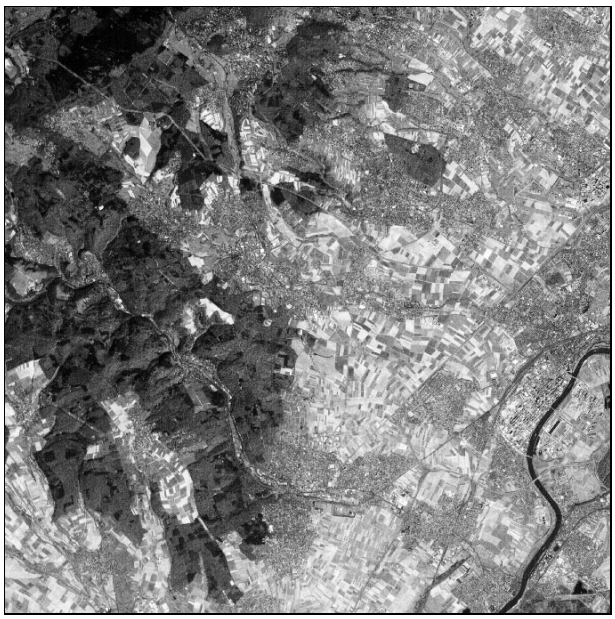

Figure 16: Part of an IRS-1C scene (2500$\times$2500 pixels) showing a site close to of Frankfurt am Main.

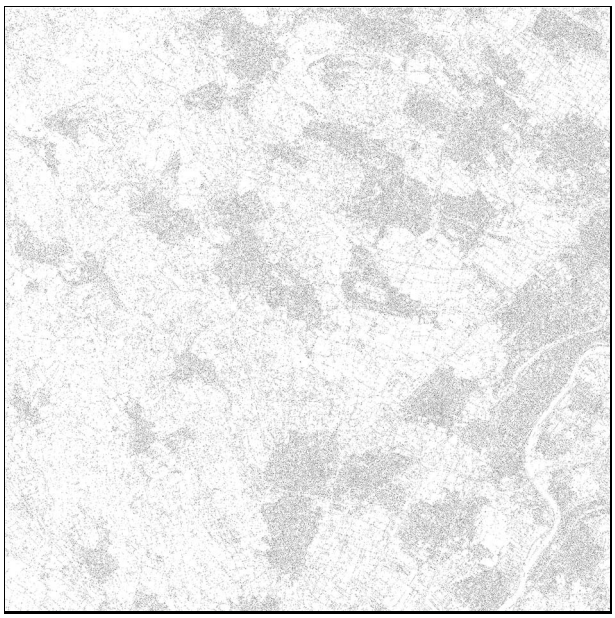

Figure 17: Significant points extracted from Fig. 16.

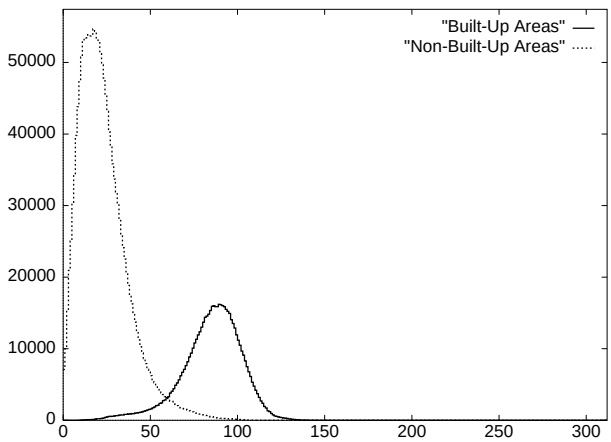

Figure 18: Feature density histograms for built-up and non-built-up areas derived from IRS data and training sites.

D. Fritsch, M. Englich & M. Sester, eds, 'IAPRS', Vol. 32/4, ISPRS Commission IV Symposium on GIS - Between Visions and Applications, Stuttgart, Germany.

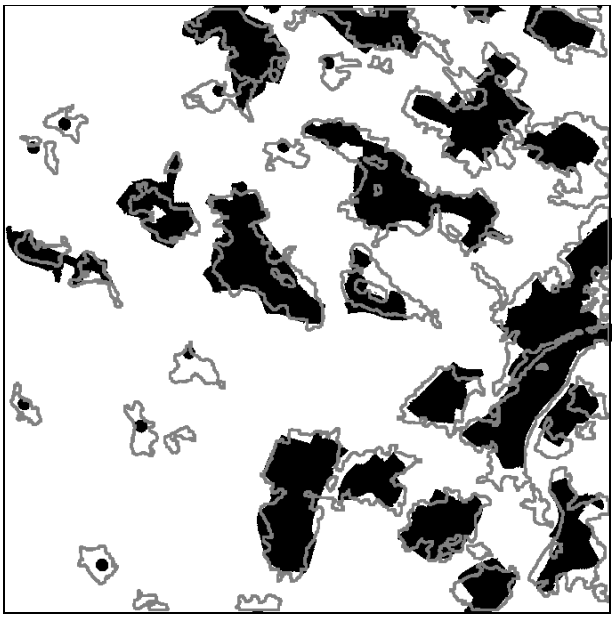

Figure 19: Detected built-up areas (grey) obtained from Fig. 16 and the GIS data (black).

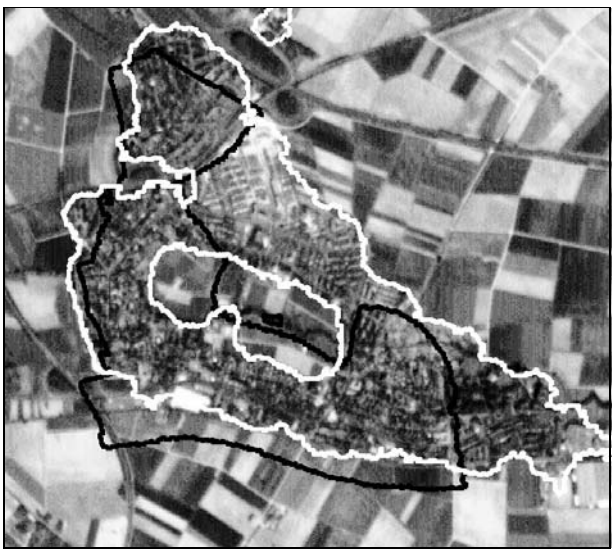

Figure 20: Detail of Fig. 16 with detected built-up areas (white) and GIS data (black).

Future work will concern the use of more than one feature, the correlation of densities of several features, decisions based on more than one thresholded feature image, and the contribution of feature density images to a texture classification jointly with other texture features. Another important goal is the development of a knowledge-based system by the incorporation of more information from the GIS to distinguish, e.g. populated places and built-up areas.

REFERENCES

Andrey, P. and Tarroux, P., 1996. Unsupervised texture segmentation using selectionist relaxation. In: Buxton and Cipolla, 1996, Vol. I, pp. 482–491.

Burghardt, D. and Meier, S., 1997. Cartographic displacement using the snakes concept. In: Förstner and Plümer, 1997, pp. 59–71.

Busch, A., 1994. Fast recognition of lines in digital images without user-supplied parameters. In: Ebner et al., 1994, pp. 91–97.

Busch, A., 1996. A common framework for the extraction of lines and edges. In: Kraus and Waldhäusl, 1996, Part B3, pp. 88–91.

Busch, A., 1997. Extraction of roads and built-up areas from satellite imagery. In: F. Leberl, R. Kalliany and M. Gruber (eds), Mapping Buildings, Roads and other Man-Made Structures from Images, Proceedings of the IAPR-TC7 Workshop ”Remote Sensing and Mapping”, Technical University Graz, Austria, 2.–3. September, 1996, Schriftenreihe der Österreichischen Computer-Gesellschaft, Vol. 92, Oldenbourg Verlag, Wien, pp. 277–292.

Buxton, B. and Cipolla, R. (eds), 1996. Computer Vision – ECCV’96, 4th European Conference on Computer Vision, Cambridge, UK, April 1996, Proceedings. Springer, Berlin.

Ebner, H., Heipke, C. and Eder, K. (eds), 1994. ISPRS Commission III Symposium: Spatial Information from Photogrammetry and Computer Vision, September 5–9, 1994, Munich, Germany. International Archives of Photogrammetry and Remote Sensing, Vol. 30, Part 3, International Society for Photogrammetry and Remote Sensing, SPIE – The International Society for Optical Engineering, Washington.

Förstner, W., 1991. Statistische Verfahren für die automatische Bildanalyse und ihre Bewertung bei der Objekterkennung und -vermessung. Deutsche Geodätische Kommission bei der Bayerischen Akademie der Wissenschaften, Reihe C, Heft Nr. 370, München.

Förstner, W. and Plümer, L. (eds), 1997. Semantic Modeling for the Acquisition of Topographic Information from Images and Maps. Birkhäuser Verlag, Basel.

Grün, A., Baltsavias, E. P. and Henricsson, O. (eds), 1997. Automatic Extraction of Man-Made Objects from Aerial and Space Images (II). Birkhäuser Verlag, Basel.

Hanke, P. and Proß, E., 1994. Zur Fortführung von ATKIS 200 unter Verwendung digitaler Bilddaten. Kartographische Nachrichten 44(4), pp. 138–143.

Haralick, R. M., 1984. Digital step edges from zero crossing of second directional derivatives. IEEE Transactions on Pattern Analysis and Machine Intelligence 6(5), pp. 58–68.

Haralick, R. M. and Shapiro, L. G., 1992. Computer and Robot Vision. Vol. 1 and 2, Addison-Wesley, Reading.

Koch, K. R. and Schmidt, M., 1994. Deterministische und stochastische Signale. Dümmler, Bonn.

D. Fritsch, M. Englich & M. Sester, eds, 'IAPRS', Vol. 32/4, ISPRS Commission IV Symposium on GIS - Between Visions and Applications, Stuttgart, Germany.

Konecny, G., 1996. International mapping from space. In: Kraus and Waldhäusl, 1996, Part B4, pp. 465–468.

Kraus, K. and Waldhäusl, P. (eds), 1996. International Society for Photogrammetry and Remote Sensing, XVIII Congress. International Archives of Photogrammetry and Remote Sensing, Vol. XXXI, Committee of the XVIIIth International Congress for Photogrammetry and Remote Sensing, Vienna, Austria.

Kunz, D., Schilling, K.-J. and Vögtle, T., 1997. A new approach for satellite image analysis by means of a semantic network. In: Förstner and Plümer, 1997, pp. 20–36.

Lohmann, G., 1991. An Evidential Reasoning Approach to the Classification of Images. DLR-Forschungsbericht, 91-29, Köln.

Lohmann, G., 1994. Assessment of textural features for remote sensing applications. In: Ebner et al., 1994, pp. 512–516.

Mecocci, A., Gamba, P., Marazzi, A. and Barni, M., 1995. Texture segmentation in remote sensing images by means of packet wavelets and fuzzy clustering. In: Proc. of the European Symposium on Satellite and Remote Sensing II, Paris, 25–29 Sept. 1995, Vol. SPIE 2584, SPIE – The International Society for Optical Engineering, Washington, pp. 142–157.

Pan, Y., 1994. Autoregressive Modelle für die Texturanalyse in digitalen Bildern. Deutsche Geodätische Kommission bei der Bayerischen Akademie der Wissenschaften, Reihe C, Heft Nr. 430, München.

Rosenfeld, A., 1998. Image analysis and computer vision: 1997. Computer Vision and Image Understanding 70(2), pp. 239–284.

Rotunno, O. C., Treitz, P. M., Soulis, E. D., Howarth, P. J. and Kouwen, N., 1996. Texture processing of synthetic aperture radar data using second-order spatial statistics. Computers & Geosciences 22(1), pp. 27–34.

Schilling, K.-J. and Vögtle, T., 1996. Satellite image analysis using integrated knowledge. In: Kraus and Waldhäusl, 1996, Part B3, pp. 752–757.

Schilling, K.-J. and Vögtle, T., 1997. An approach for the extraction of settlement areas. In: Grün et al., 1997, pp. 333–342.

Shao, J. and Förstner, W., 1994. Gabor wavelets for texture edge extraction. In: Ebner et al., 1994, pp. 745–752.

Vögtle, T. and Schilling, K.-J., 1995. Wissensbasierte Extraktion von Siedlungsbereichen in der Satellitenbildanalyse. Zeitschrift für Photogrammetrie und Fernerkundung 63(5), pp. 199–207.

Xie, Z.-Y. and Brady, M., 1996. Texture segmentation using local energy in wavelet scale space. In: Buxton and Cipolla, 1996, Vol. I, pp. 304–313.